

Spin-resolved photoemission from submonolayer Ag on Si(111): Ag adsorption in the $(\sqrt{3} \times \sqrt{3})R30^\circ$ phase with no Ag-Ag interaction and in the 1×1 structure with strong Ag-Ag interaction

B. Vogt, B. Schmiedeskamp, and U. Heinzmann

*Fakultät für Physik, Universität Bielefeld, Postfach 8640, D-4800 Bielefeld 1, Federal Republic of Germany
and Fritz-Haber-Institut der Max-Planck-Gesellschaft, Faradayweg 4-6, D-1000 Berlin 33, Federal Republic of Germany*

(Received 24 May 1990)

Ag/Si(111) has been studied by spin-, angle-, and energy-resolved photoemission with circularly polarized radiation of Berliner Elektronenspeicherring-Gesellschaft für Synchrotronstrahlung (BESSY) for the 1×1 and the $(\sqrt{3} \times \sqrt{3})R30^\circ$ surface at a coverage of 0.5 monolayer. The spin-resolved photoemission data were obtained for normal incidence of the light and normal emission of the photoelectrons. For both the 1×1 and the $(\sqrt{3} \times \sqrt{3})R30^\circ$ structure we find no dispersion in the Ag photoelectron peaks depending on K_{\parallel} and K_{\perp} . For the 1×1 structure and for photon energies between 20 and 24 eV we observe an additional Ag photoelectron peak at about 1 eV higher binding energy which results from a d -level splitting due to Ag-Ag interaction. This peak is absent for the $(\sqrt{3} \times \sqrt{3})R30^\circ$ phase, which demonstrates that the Ag-Ag neighbor interaction is negligible. This supports the models which do not imply Ag-Ag interaction for Ag adsorption in the $(\sqrt{3} \times \sqrt{3})R30^\circ$ phase.

Ag/Si(111) has been studied several times in the past with different techniques.¹⁻²² For Ag deposition at room temperature on Si(111) one obtains the 1×1 structure in the submonolayer regime. Based on different experiments it is now commonly believed that Ag grows in two-dimensional (2D) islands with Ag-monolayer thickness up to coverages of about 0.7 layer.^{1,2} Deposition at or heating to temperatures between 200 and 500 °C after deposition yields a $(\sqrt{3} \times \sqrt{3})R30^\circ$ low-energy electron diffraction (LEED) pattern. Different models have been proposed for this phase. Some authors base their model on a Ag honeycomb arrangement slightly embedded below the first Si layer.⁵⁻¹⁰ They are supported by ISS (ion surface scattering),⁵ LEED,⁶ surface extended x-ray-absorption fine structure (SEXAFS),⁷ Auger-electron spectroscopy (AES) and LEED,⁸ and ultraviolet photoelectron spectroscopy^{9,10} (UPS) experiments. Some scanning tunneling microscopy (STM) experiments point to a Ag/Si(111) $(\sqrt{3} \times \sqrt{3})R30^\circ$ phase as a Ag honeycomb above the first Si layer.^{11,12} A third model is assuming an ordered Ag trimer embedded in a Si honeycomb.^{13,14,18-21} The support comes from UPS and AES studies,^{13,14} STM experiments,¹⁸ ICISS (impact-collision ion scattering),¹⁹ and surface x-ray diffraction.²⁰ The very recent experiments with the same STM technique favor different models: a Ag trimer model¹⁸ and a Ag honeycomb model.^{11,12} Dynamical LEED data²² result in an interpretation where the Si atoms are responsible for the $(\sqrt{3} \times \sqrt{3})R30^\circ$ LEED pattern and where the Ag is adsorbed in a "dilute" phase. This is supported by the fact that even a clean Si surface can show a $(\sqrt{3} \times \sqrt{3})R30^\circ$ LEED pattern under certain conditions.^{22,23} While the last model excludes a long-range ordering of the Ag atoms, all other models described above contain such an ordering.

The authors have performed spin-resolved photoemis-

sion experiments for the 1×1 and the $(\sqrt{3} \times \sqrt{3})R30^\circ$ structure. The splittings, shifts, and spin polarization of the Ag peaks in the photoemission spectra are investigated in order to gain information in regard to the electronic structures of the Ag adsorbates which are often strongly related to the geometric ordering of the Ag atoms. Ag-Ag interaction in ordered structures is expected to yield peak splittings while this is not expected for noninteracting Ag atoms in a dilute phase. The advantage of spin-polarized photoemission with circularly polarized radiation, as used in these studies, is its unique capability of identifying peak splittings with a high degree of certainty, if the spin-orbit interaction affects the splitting mechanism.

The experiments were performed at the 6.5-m normal-incidence vuv monochromator²⁴ at Berliner Elektronenspeicherring-Gesellschaft für Synchrotronstrahlung (BESSY) with circularly polarized off-plane radiation. The apparatus used for the measurements has been described previously,²⁵ an evaporator was added.

All photoemission data were obtained for normal incidence of the circularly polarized radiation. The photoelectrons were analyzed with respect to their kinetic energy and emission angle θ by an electron spectrometer.²⁶ The overall energetic resolution (electrons plus photons) was better than 200 meV at an angular resolution of $\pm 3^\circ$ (geometric resolution).

The surface normal of the Si(111) crystal which was a cut wafer of 0.25 mm thickness coincided with 0.5° with the [111] direction and within 0.3° with the light direction. The crystal surface was covered with a SiO₂ layer. The clean Si-crystal surface was prepared by heating up to 1000 °C. It was controlled by Auger-electron spectroscopy (AES) and LEED. The evaporation was performed with a resistively heated Ag evaporator while the substrate remained at room temperature. The oven was placed ≈ 20 cm away from the target. The Ag beam was

geometrically collimated by a small tube. After an initial outgasing the evaporator worked without deterioration of the UHV conditions (base pressure in the 10^{-10} mbar range). The oven was used for short periods, in between the surface was controlled by LEED and AES.

The result, in general, of the coverage dependence of the spin-resolved photoemission and a description of the coverage calibration with Auger-electron spectroscopy will be published elsewhere.²⁷ Here only the photoemission studies at a Ag coverage of 0.5 monolayer are presented. When Ag was deposited at room temperature a 1×1 LEED pattern was recorded. This layer was first studied by spin-resolved photoemission. Then the crystal was heated to about 500°C and a $(\sqrt{3} \times \sqrt{3})R30^\circ$ LEED pattern was observed, followed again by a photoemission study. Typical intensities of the photoelectron spectra for the Ag adsorbate in the $(\sqrt{3} \times \sqrt{3})R30^\circ$ phase and in the 1×1 structure for normal radiation incidence and an electron emission angle of $\theta = 25^\circ$ are shown in the left-hand side of Fig. 1. The peak at ≈ 5 eV below E_F can be identified as a d -derived Ag peak, because its energetic position is close to that obtained for Ag/Pt(111).²⁸ The center of this peak was determined for a series of energies between 11 and 19 eV and several emission angles between 0° and 45° . The resultant dispersions of the Ag intensity peak for the 1×1 and the $(\sqrt{3} \times \sqrt{3})R30^\circ$ surface are shown in the right-hand side of Fig. 1. In the lower right-hand side of Fig. 1 the dispersion along the ΓH direction which is the bisector of the angle between the ΓM and the ΓK direction of the surface Brillouin zone is presented. For both, variation of K_{\parallel} (lower part) and K_{\perp} (upper part), within the experimental uncertainty the same energetic position of the peak for all spectra of the 1×1 and for all spectra of the $(\sqrt{3} \times \sqrt{3})R30^\circ$ surface was found. This indicates a 2D growth in both cases. In re-

gard to the left-hand side of Fig. 1 the spectra for the 1×1 and the $(\sqrt{3} \times \sqrt{3})R30^\circ$ surface show that the peak shape and full width at half maximum of the Ag peak in the range of 5 and 6 eV below E_F are very similar. The spectra differ however by a 0.3 eV shift of the peak maxima and in the intensity of secondary electrons [a strong peak for the 1×1 structure at 11 eV binding energy, no such peak for the $(\sqrt{3} \times \sqrt{3})R30^\circ$ phase]. These results already show that the two studied systems differ significantly regarding their electronic structure.

The comparison of the photoemission spectra for the two phases is continued in more detail with the data given in Figs. 2 and 3 for the 1×1 structure and the $(\sqrt{3} \times \sqrt{3})R30^\circ$ phase, respectively. These data were obtained for normal radiation incidence and normal electron emission.

In the left-hand side of Fig. 2 photoelectron intensities for $h\nu = 19$ eV up to $h\nu = 24$ eV are shown. Only one peak for photon energies below 21 eV was observed. Around $h\nu = 23$ eV one additional structure occurs in the photoelectron spectra at higher binding energies. Spin-resolved photoemission is used to identify their nature. In the right-hand side of Fig. 2 spin-resolved intensities I_+ and I_- for the 1×1 structure are shown for 19 and 23 eV photon energy. I_+ and I_- denote the intensity of the electrons with spin parallel and antiparallel to the photon spin, respectively, and are obtained from the total intensity I and the measured spin polarization P by means of the equations $I_{+/-} = \frac{1}{2} I(1 \pm P)$. For $h\nu = 19$ eV (lower spectrum) we find the spin-orbit splitting of the d -derived peak which was already used for the mapping in Fig. 1.

At the photon energy of $h\nu = 23$ eV two additional peaks occur in the spin-resolved intensities. The spin-polarization sign of the peak at ≈ 5 eV below E_F shows a $-/+$ sequence, which inverts to $+/-$ for the peak at

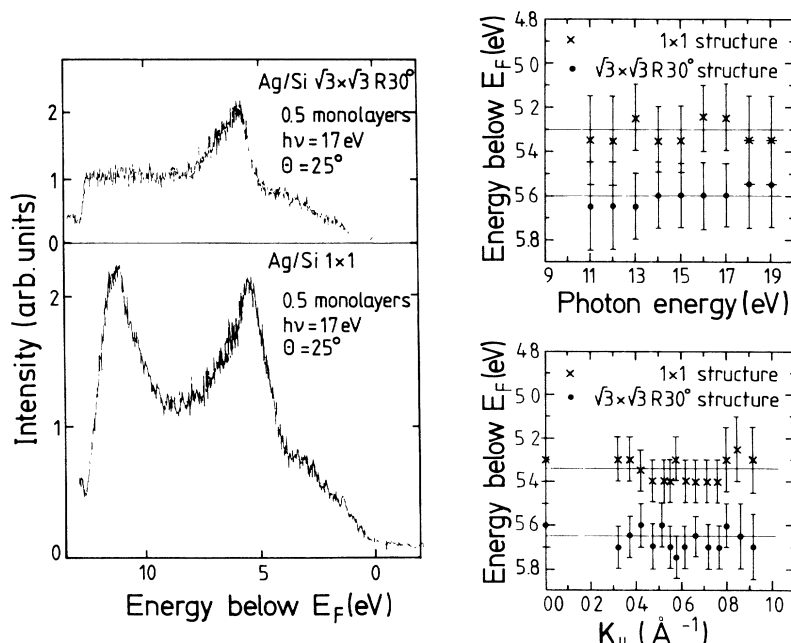


FIG. 1. Photoemission from the 1×1 and the $(\sqrt{3} \times \sqrt{3})R30^\circ$ surface. Left-hand side: typical intensity spectra. Right-hand side: dispersion in the K_{\parallel} and K_{\perp} direction.

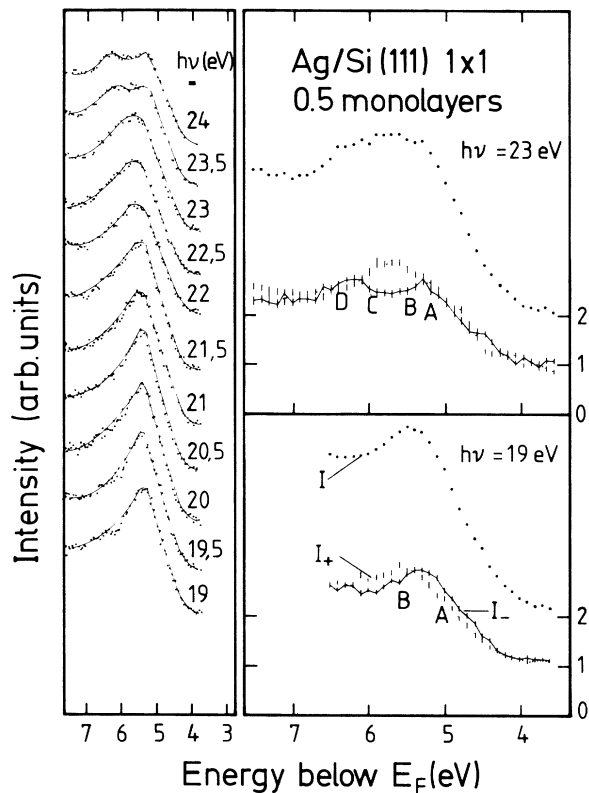


FIG. 2. Photoemission intensities for $h\nu=19$ eV up to $h\nu=24$ eV from the 1×1 structure. Left-hand side: photon energy dependence. Right-hand side: spin-resolved intensities for $h\nu=19$ and 23 eV.

≈ 6 eV below E_F . This result was also observed and studied in detail recently for ultrathin epitaxial Ag layers²⁸ on Pt(111). For these epitaxial systems the Ag-Ag distance is almost identical with the Ag bulk value and the additional peak was assigned to collective Ag-Ag interaction. It is the same mechanism which splits the two spin-orbit levels of a free Ag atom into two pairs of spin-orbit split levels when forming a solid. The occurrence of these peaks for the 1×1 phase is surprising, since it appears to be in contradiction to some existing models for the 1×1 phase in the submonolayer regime (Ref. 1 and references therein). These models assume a 2D Ag-island growth where the Ag atoms are packed commensurably with the Si(111) substrate with a Ag-Ag distance of 3.84 Å up to a coverage of $\frac{2}{3}$ monolayers. Since it is improbable that a bulklike Ag-Ag interaction can be built up over these large distances (in the bulk the Ag atoms are separated by only 2.9 Å), our data support the models with shorter bulklike Ag-Ag distances which are proposed for higher coverages above $\frac{2}{3}$ monolayers,^{1,5} by extending their validity to our 0.5 layer Ag adsorbate.

The photoemission spectra of the $(\sqrt{3}\times\sqrt{3})R30^\circ$ structure were studied to search for the two peaks at about 6 eV binding energy. The results are given in Fig. 3. The left-hand side of Fig. 3 presents intensity spectra for photon energies between 19 and 24 eV, the right-hand side the corresponding spin-resolved data for two photon energies. Only one spin-orbit split peak was observed. Fur-

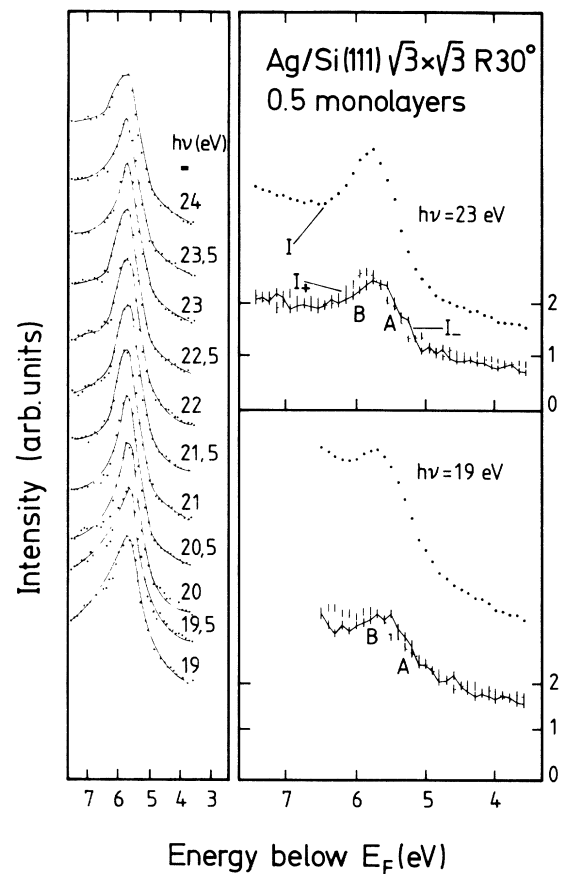


FIG. 3. Photoemission intensities for $h\nu=19$ eV up to $h\nu=24$ eV from the $(\sqrt{3}\times\sqrt{3})R30^\circ$ phase. Left-hand side: photon-energy dependence. Right-hand side: spin-resolved intensities for $h\nu=19$ and 23 eV.

ther structures as those revealed for the 1×1 structure in Fig. 2 are not visible.

Based on the intensity spectra only one might argue that though the total energy width of the Ag photoemission peak is considerably smaller than for a 3D Ag crystal, it is still larger than the width obtained in a photoionization experiment with free Ag atoms,²⁹ and one might interpret this difference in the peak width as being due to a small Ag-Ag interaction (this interpretation has indeed been given in Ref. 10 to interpret nonspin resolved photoemission data). If this was true the spin-resolved photoemission spectrum for $h\nu=23$ eV in Fig. 3 should show a broadening of the I_- peak at A due to the development of an I_- peak at D at the low-energy edge of peak B. We note, however, neither an indication of an I_- peak at the low-energy side of peak B, nor a difference in peak shape of the I_+ and I_- peaks in Fig. 3. The Ag-Ag interaction in the $(\sqrt{3}\times\sqrt{3})R30^\circ$ phase is thus at least an order of magnitude smaller than in bulk Ag and the 1×1 phase. These experimental results favor the models for the Ag adsorption in the $(\sqrt{3}\times\sqrt{3})R30^\circ$ phase discussed in the literature¹⁻²² which do not imply Ag-Ag interaction. The requirement of the missing Ag-Ag interaction is, of course, given for a dilute Ag adsorption on a $(\sqrt{3}\times\sqrt{3})R30^\circ$ Si surface.²² This does not exclude other

models which propose certain Ag-adsorption sites without Ag-Ag interaction. It should, however, be noted that a long-range ordering of the Ag atoms on Si(111) is not caused by Ag-Ag interaction.

We studied the spin-resolved photoemission from Ag/Si(111) for the 1×1 structure and from the $(\sqrt{3} \times \sqrt{3})R30^\circ$ phase at the same coverage of 0.5 monolayer. For both phases the binding energy of the first Ag peak below E_F in the photoemission spectra does not depend on the photon energy or the emission angle, i.e., we find no band dispersion. A considerable difference in the spectra is found for photon energies between 21 and 24 eV. For the 1×1 structure we find an additional intensity peak at 1 eV higher binding energy due to Ag-Ag interaction, which has approximately the same size as in a 3D Ag

crystal. This favors the model of 2D island growth for the 1×1 phase. The splitting is at least an order of magnitude smaller in the spectra for the $(\sqrt{3} \times \sqrt{3})R30^\circ$ phase as could be shown by means of the spin-resolved photoemission spectra. Our data strongly favor an adsorption model for the $(\sqrt{3} \times \sqrt{3})R30^\circ$ phase, which does not imply Ag-Ag interaction.

We appreciate discussions with N. Irmer, N. Müller, and P. Stoppmanns as well as the support of the BESSY staff. The authors would also like to thank M. Fink for a careful reading of the manuscript. This work was financially supported by the Bundesministerium für Forschung und Technologie (BMFT) Grant No. 5431, Bonn, Germany.

-
- ¹G. Le Lay, *Surf. Sci.* **132**, 169 (1983), and references therein.
²M. Hanbücken, M. Futamoto, J. A. Venables, *Surf. Sci.* **147**, 433 (1984).
³E. J. Van Loenen, M. Iwami, R. M. Tromp, and J. V. Van der Veen, *Surf. Sci.* **137**, 1 (1984).
⁴J. A. Venables, J. Derrien, and A. P. Janssen, *Surf. Sci.* **95**, 411 (1980).
⁵M. Saitoh, F. Shoji, K. Oura, and T. Hanawa, *Surf. Sci.* **112**, 306 (1981).
⁶Y. Terada, T. Yoshizuka, K. Oura, and T. Hanawa, *Surf. Sci.* **114**, 65 (1982).
⁷J. Stör, R. Jaeger, G. Rossi, T. Kendelewicz, and I. Lindau, *Surf. Sci.* **134**, 813 (1983).
⁸G. Le Lay, M. Manneville, and R. Kern, *Surf. Sci.* **72**, 405 (1978); G. Le Lay, A. Chauvel, M. Manneville, and R. Kern, *Appl. Surf. Sci.* **9**, 190 (1981).
⁹F. Houzay, G. M. Guichar, A. Cros, F. Salvan, R. Pinchaux, and J. Deuvien, *Surf. Sci.* **124**, L1 (1989).
¹⁰K. Markert, P. Pervan, W. Heichler, and K. Wandelt, *J. Vac. Sci. Technol.* **A7**, 2873 (1989).
¹¹R. J. Wilson and S. Chiang, *Phys. Rev. Lett.* **58**, 369 (1987).
¹²R. J. Wilson and S. Chiang, *Phys. Rev. Lett.* **59**, 2329 (1987).
¹³F. Wehking, H. Beckermann, and R. Niedermayer, *Surf. Sci.* **71**, 364 (1978).
¹⁴G. V. Hansson, R. Z. Bachrack, R. S. Bauer, and P. Chiradin, *Phys. Rev. Lett.* **46**, 1033 (1981); *J. Vac. Sci. Technol.* **18**, 550 (1981).
¹⁵T. Yokotsuka, S. Kono, S. Suzuki, and T. Sagawa, *Surf. Sci.* **127**, 35 (1983).
¹⁶S. Kono, K. Higashiyama, and T. Sagawa, *Surf. Sci.* **165**, 21 (1986).
¹⁷D. Bolmont, Ping Chen, and C. A. Sebenne, *J. Phys. C* **14**, 3313 (1981).
¹⁸E. J. van Loenen, J. E. Demuth, R. M. Tromp, and R. J. Hamers, *Phys. Rev. Lett.* **58**, 373 (1987).
¹⁹T. L. Porter, C. S. Chang, and I. S. T. Tsong, *Phys. Rev. Lett.* **60**, 1739 (1988).
²⁰E. Vlieg, A. W. Denier van der Gon, and J. F. Van der Veen, *Surf. Sci.* **209**, 100 (1989).
²¹L. S. D. Johansson, E. Landemark, C. J. Karlsson, and R. I. G. Uhrberg, *Phys. Rev. Lett.* **63**, 2092 (1989).
²²W. C. Fan, A. Ignatiev, H. Huang, and S. Y. Tong, *Phys. Rev. Lett.* **62**, 1516 (1989).
²³W. S. Yang, S. C. Wu, and F. Jona, *Surf. Sci.* **169**, 383 (1986).
²⁴F. Schäfers, W. Peatman, A. Eyers, Ch. Heckenkamp, G. Schönhense, and U. Heinzmann, *Rev. Sci. Instrum.* **57**, 1032 (1986).
²⁵A. Eyers, F. Schäfers, G. Schönhense, U. Heinzmann, H. P. Oepen, K. Hünlich, J. Kirschner, and G. Borstel, *Phys. Rev. Lett.* **52**, 1559 (1984).
²⁶K. Jost, *J. Phys. E* **12**, 1001 (1979); **12**, 1006 (1979).
²⁷B. Schmiedeskamp, B. Vogt, and U. Heinzmann (unpublished).
²⁸B. Schmiedeskamp, B. Kessler, B. Vogt, and U. Heinzmann, *Surf. Sci.* **223**, 465 (1989).
²⁹J. M. Dyke, N. K. Fayad, A. Morris, and I. R. Trickle, *J. Phys. B* **12**, 2985 (1979).